

# The reflectance spectra of opal-A (0.5–25 $\mu\text{m}$ ) from the Taupo Volcanic Zone: Spectra that may identify hydrothermal systems on planetary surfaces

Michelle C. Goryniuk, Benoit A. Rivard, and Brian Jones

Department of Earth and Atmospheric Sciences, University of Alberta, Edmonton, Alberta, Canada

Received 13 September 2004; accepted 26 October 2004; published 16 December 2004.

[1] Opal-A, the main component of siliceous sinters in many terrestrial hydrothermal systems, is a hydrated silicate that commonly incorporates silicified microorganisms. The detection of opal-A on the surface of Mars, therefore, may carry important implications in the search for extraterrestrial life. Sintors from the discharge apron of Ohaaki Pool (North Island, New Zealand) yielded reflectance spectra (wavelengths between 0.5–25  $\mu\text{m}$ ) that indicate the presence of absorbed water, trapped water, and silanol in opal-A. Two classes (1 and 2) of reflectance spectra were detected between the wavelengths of 6–13  $\mu\text{m}$ . The Class-1 spectrum is similar to existing opal spectra, and was collected from well-consolidated samples that had low porosity. The Class-2 spectrum is unique when compared to the spectra of other silica polymorphs, and was collected from poorly consolidated samples that had high porosity. **INDEX TERMS:** 3934 Mineral Physics: Optical, infrared, and Raman spectroscopy; 5460 Planetology: Solid Surface Planets: Physical properties of materials; 5464 Planetology: Solid Surface Planets: Remote sensing; 6225 Planetology: Solar System Objects: Mars. **Citation:** Goryniuk, M. C., B. A. Rivard, and B. Jones (2004), The reflectance spectra of opal-A (0.5–25  $\mu\text{m}$ ) from the Taupo Volcanic Zone: Spectra that may identify hydrothermal systems on planetary surfaces, *Geophys. Res. Lett.*, 31, L24701, doi:10.1029/2004GL021481.

## 1. Introduction

[2] Opal-A ( $\text{SiO}_2 \cdot n\text{H}_2\text{O}$ ), which is composed of silica spheres 1500–3000 Å in diameter [Rodgers *et al.*, 2004], is a hydrated silica (1–15.6 wt. %  $\text{H}_2\text{O}$ ) characterized by silanol (OH attached to Si), absorbed water attached to silanol, and/or water that is trapped between the silica beads [Jones and Renaut, 2004]. Opal-A is the dominant component of siliceous sinters that are found on the discharge aprons around modern geysers and hot springs. Such sinters commonly contain numerous microorganisms that have been replaced and encrusted by opal-A [Jones *et al.*, 1998]. Thus, detection of opal-A on any planetary surface, including Mars, may carry important implications in the search for extraterrestrial life.

[3] Michalski *et al.* [2003] showed that silica polymorphs (opal, tridymite, cristobalite, quartz and coesite) are spectrally distinguishable at high resolutions. It is difficult, however, to differentiate between the opaline phases (opal-A, opal-CT, opal-C) because they are spectrally similar. The main theme of this paper is the discovery of two classes of opal-A

spectral signatures, one that resembles the opal-A spectrum presented by Michalski *et al.* [2003], and another spectrum that is distinct from other silica polymorphs, which has not been previously documented. The discovery of this new opal-A spectrum is significant because it came from opal-A deposits that have high porosity. If identified on the surface of Mars, the spectrum would indicate the presence of opal-A that has not been exposed to extensive secondary silica precipitation.

## 2. Materials and Methods

### 2.1. Site Description

[4] Samples of siliceous sinter were collected from the discharge apron around Ohaaki Pool (~45 m long and ~15 wide), which is located in the Taupo Volcanic Zone on the North Island of New Zealand [Jones *et al.*, 1998]. The sinters were precipitated from discharged alkaline  $\text{Na-HCO}_3\text{-Cl}$  dilute spring waters at 95°C [Mahon and Finlayson, 1972]. Mineralogy was confirmed by x-ray diffraction of powdered cavity mounts using a Rigaku rotating anode-diffractometer, and by SEM analysis of the morphology of the precipitates [Jones *et al.*, 1998].

### 2.2. Description of Samples

[5] Four hand samples (NZ152, NZ313, NZ341, and NZ413) and 10 cores were examined. NZ313 and NZ341 were poorly consolidated and characterized by visible porosity. NZ152 was a more consolidated sample and showed no visible porosity. The basal part of NZ413 was consolidated, whereas the upper part was formed of less consolidated and more porous material. The cores are characterized by thin horizontal laminations (1–5 mm thick), which are the result of biotic and abiotic processes [Jones *et al.*, 1998; Jones and Renaut, 2004].

### 2.3. Instrumentation Setup

[6] Bidirectional reflectance measurements from the wavelengths between 2.5–22  $\mu\text{m}$  were collected from cut and natural surfaces of hand samples using a Bomem MB102 Fourier transform infrared (FTIR) spectrometer. Using a global light source, and a viewing angle of 35°, measurements were collected at a resolution of 16  $\text{cm}^{-1}$ , with a field of view of approximately 4 × 4 mm. The measurements were collected from flat surfaces along continuous linear transects. Thirty-two scans (for one spectrum) were made in each location, then the sample was moved ~5 mm and another measurement was taken. The same samples were also analyzed using the ASD field spec FR, which collected reflectance spectra from 0.4–2.5  $\mu\text{m}$ .

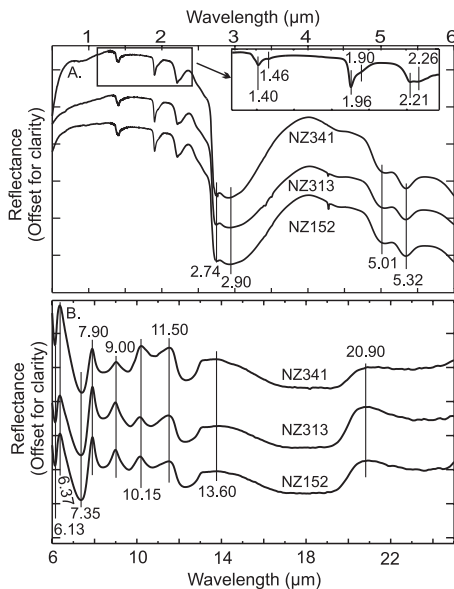


**Figure 1.** The spectral features of opal-A documented between the wavelengths of 0.5–6  $\mu\text{m}$  (a), and 6–25  $\mu\text{m}$  (b), collected from samples NZ152, NZ313, and NZ341, grain size fraction <74  $\mu\text{m}$ . Measurements were collected using a UV-VIS-NIR Bidirectional Spectrometer (0.32–1.8  $\mu\text{m}$ ) and a Nicolet Nexus 870 FT-IR Spectrometer (1.8–26  $\mu\text{m}$ ).

[7] Analyses of loose crushed material were carried out at the Reflectance Experiment Laboratory (RELAB) at Brown University, Rhode Island, using a UV-VIS-NIR Bidirectional Spectrometer (0.32–1.8  $\mu\text{m}$ , incidence/emergence angles at 30° and 0°) and a Nicolet Nexus 870 FT-IR Spectrometer (1.8–26  $\mu\text{m}$ ).

### 3. Results and Discussion

#### 3.1. Band Assignment

##### 3.1.1. Spectral Features in the Range of 0.5–7.0 $\mu\text{m}$

[8] The major spectral features of opal-A, related to the presence of OH and H<sub>2</sub>O, are located at 1.40, 1.46, 1.90, 1.96, 2.21, 2.26, 2.74, 2.90, 5.01, 5.32, 6.13, and 6.37  $\mu\text{m}$  (Figure 1a and Table 1) [Langer and Florke, 1974; Hunt, 1977; Salisbury et al., 1991a, 1991b; Dijkstra et al., 2002].

[9] Sharp troughs at 1.40 and 1.90  $\mu\text{m}$  are consistent with isolated H<sub>2</sub>O and OH that exist in similar positions in the crystalline environment. Troughs at 1.46 and 1.96  $\mu\text{m}$  are assigned to H-bound H<sub>2</sub>O and OH. At 2.21 and 2.74  $\mu\text{m}$ , and at 2.26 and 2.90  $\mu\text{m}$ , are the stretching and bending modes of isolated and H-bound silanol, respectively. Troughs at 5.01 and 5.32  $\mu\text{m}$  are assigned to the overtones of H<sub>2</sub>O and OH whereas the trough at 6.13  $\mu\text{m}$  and the peak at 6.37  $\mu\text{m}$  are due to isolated molecular H<sub>2</sub>O.

[10] These observations are consistent with the model of Langer and Florke [1974] and Adams et al. [1991] where H<sub>2</sub>O is found trapped as isolated molecules free from H-bonding and as liquid water in which the molecules are hydrogen bonded to other H<sub>2</sub>O molecules. This model also includes the presence of –OH bonded to silicon either

interacting with water on the surface, or protected from interaction with water [Frondel, 1982].

##### 3.1.2. Spectral Features in the Range of 7–25 $\mu\text{m}$

[11] For opal-A, the major spectral features at 7.90, 9.00, 10.15, 11.50, 13.60, and 20.90  $\mu\text{m}$  (Figure 1b and Table 1), are related to the fundamental vibrational frequencies of the Si-O stretch and bend [McDonald, 1958; Lyon, 1967; Salisbury and Walter, 1989].

[12] The Christiansen Feature (CF) for opal-A is located at 7.35  $\mu\text{m}$ . The CF for silicates commonly falls between 7.5–9  $\mu\text{m}$  [Salisbury et al., 1991b], but can go as low as 7.35 for the silica polymorphs [Michalski et al., 2003]. The Reststrahlen band at 7.90  $\mu\text{m}$ , which is positioned at a shorter wavelength than any Reststrahlen band observed in other silica phases [Hunt and Salisbury, 1970; Hunt et al., 1973], could be the result of a shorter Si-O bond length, and a larger Si-O-Si angle than that of quartz [Gibbs, 1982; Pauling, 1980; Smith and Bailey, 1963]. The Reststrahlen band at 9.00  $\mu\text{m}$  is characteristic of the major bands for tectosilicates, which typically occur at wavelengths close to 9.1  $\mu\text{m}$ .

[13] Two peaks at 10.15 and 11.50  $\mu\text{m}$  are attributed to the Si-O stretch of the Si-O bond of the terminal oxygens of silanol [Moenke, 1974], and the peak at 10.15  $\mu\text{m}$  is a common feature in spectra for diatoms and other types of opaline silica [Sun, 1962; Chester and Elderfield, 1968; Moenke, 1974]. The amplitude of the peak at 11.50  $\mu\text{m}$  varies directly with the amplitude of the band at 10.15  $\mu\text{m}$ , and therefore can also be attributed to silanol. Although these two features have been observed in the spectra of silicates that have been subjected to vigorous grinding [Takamura et al., 1964], we know of no other study describing the presence of these two features in spectra from natural surfaces.

[14] The transparency feature at 13.60  $\mu\text{m}$ , and a single Si-O-Si bending vibration is located at 20.90  $\mu\text{m}$ , with the

**Table 1.** The Position of Spectral Features for NZ152 Between 0.5–25  $\mu\text{m}$  (Grain Size 0–74  $\mu\text{m}$ ), Correlated With the Vibrational Movement of the Active Molecule

$\lambda$ ( $\mu\text{m}$ )	Vibrational Movement	Active Molecule
1.40	Overtone of –OH stretch	H <sub>2</sub> O and OH <sup>a,b,c</sup>
1.46	Overtone of –OH stretch	OH <sup>d</sup>
1.90	–OH stretch, H-O-H bend	Isolated H <sub>2</sub> O <sup>a,b,c</sup>
1.96	–OH stretch	H-Bound H <sub>2</sub> O <sup>d</sup>
2.21	–OH stretch, Si–OH bend	Isolated Si-OH <sup>a,c</sup>
2.26	–OH stretch, Si–OH bend	H-bound Si-OH <sup>a,c</sup>
2.74	–OH stretch (sym.)	Isolated Si-OH <sup>c</sup>
2.90	–OH stretch (asym.)	H-bound Si-OH <sup>c</sup>
5.01	Overtone (H <sub>2</sub> O, OH <sup>–</sup> )	H <sub>2</sub> O, OH <sup>f</sup>
5.32	Overtone (H <sub>2</sub> O, OH <sup>–</sup> )	H <sub>2</sub> O, OH <sup>f</sup>
6.13	H-O-H bend	H <sub>2</sub> O <sup>a</sup>
7.35	Christensen Frequency	— <sup>g</sup>
7.90	Si-O stretch (asym.)	Si-O-Si <sup>f,g</sup>
9.00	Si-O stretch (asym.)	Si-O-Si <sup>h</sup>
10.15	Si-O stretch	Isolated Si-OH <sup>h</sup>
11.50	Si-O stretch	H-Bound Si-OH <sup>h</sup>
13.60	Transparency Features	— <sup>g</sup>
20.90	Si-O-Si bend (asym.)	Si-O-Si <sup>i</sup>

<sup>a</sup>Aines and Rossman [1984].

<sup>b</sup>Hunt [1977].

<sup>c</sup>McDonald [1958].

<sup>d</sup>Langer and Florke [1974].

<sup>e</sup>Dijkstra et al. [2002].

<sup>f</sup>Salisbury et al. [1991b].

<sup>g</sup>Salisbury and Walter [1989].

<sup>h</sup>Moenke [1974].

<sup>i</sup>Milkey [1960].

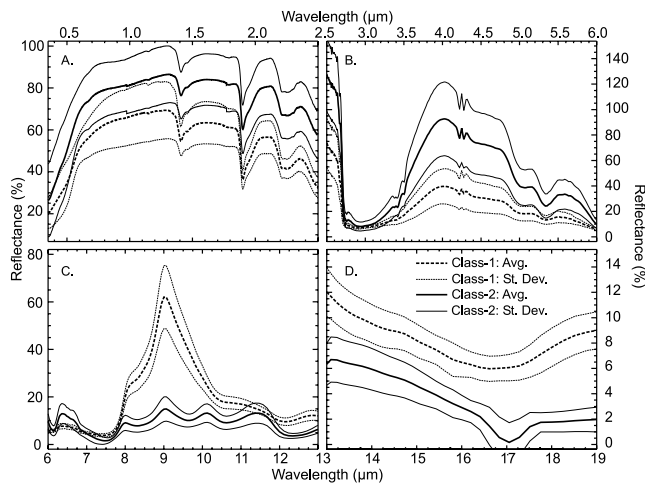


**Figure 2.** The average Class-1 and Class-2 spectra from NZ152, NZ313, NZ341, and NZ413, between 0.5–2.5  $\mu\text{m}$  (a), 2.5–6.0  $\mu\text{m}$  (b), 6.0–13.0  $\mu\text{m}$  (c), 13.0–19.0  $\mu\text{m}$  (d). Spectra were manually placed into a class, and then an average and standard deviation were calculated for each of the classes. Measurements were collected using an ASD Fieldspec (0.1–2.5  $\mu\text{m}$ ), and a Bomem MB102 FTIR (2.5–22  $\mu\text{m}$ ).

shape of this last feature being consistent with poorly ordered material [Milkey, 1960].

### 3.2. Two Spectral Classes

[15] Between the wavelengths of 6–13  $\mu\text{m}$ , two classes of spectra (Class 1 and 2) were observed in hand samples, cores, and crushed materials (Figure 2c). The two classes were characterized by changes in the relative intensities of the bands at 6.37, 7.90, 9.00, 10.15, and 11.37  $\mu\text{m}$ , and by the amplitude of the entire spectrum between 6–13  $\mu\text{m}$ . The two classes were not distinguishable below 6  $\mu\text{m}$ , however Class-1 spectra, on average, had lower amplitudes than Class-2 (Figures 2a and 2b).

[16] Class-1 spectra have a weak peak at 6.37  $\mu\text{m}$ , strong peaks at 7.90 and 9.00  $\mu\text{m}$ , absent or very weak peaks between 10–12  $\mu\text{m}$ , and a spectrum with large amplitude. Class-2 spectra have a strong peak at 6.37  $\mu\text{m}$ , weaker peaks at 7.90 and 9.00  $\mu\text{m}$ , two moderate peaks between 10–12  $\mu\text{m}$ , and a spectrum with low amplitude. Among 77 spectra that were collected from four hand samples, 12 were Class-1 spectra, and 65 were Class-2.

### 3.3. Effect of Physical Properties on Reflectance Spectra

[17] The two classes of opal-A spectra, first collected from whole and uncrushed hand samples, probably reflect differences in physical properties, such as grain size and porosity, relating to the amount of silica cement precipitated in the pore spaces. To test this, three hand samples (NZ152, NZ313, NZ341) and one core sample (OP7) were crushed to three different grain sizes (0–74  $\mu\text{m}$ , 74–250  $\mu\text{m}$ , and 250–500  $\mu\text{m}$ ). Hunt [1977] and Salisbury *et al.* [1991a] have extensively documented the effects that grain size and porosity have on reflectance spectra.

[18] Uncrushed hand samples of well consolidated material with low porosity (NZ152 and OP7) produced Class-1

spectra. These samples were well consolidated and had low porosity because silica cement had filled the pore spaces between the silica spheres. After crushing, grain size fractions >74  $\mu\text{m}$  yielded Class-1 spectra, whereas grain size fractions <74  $\mu\text{m}$  produced Class-2 spectra (Figure 3).

[19] Uncrushed hand samples of poorly consolidated material with high porosity (NZ313 and NZ341) produced Class-2 spectra. These samples were poorly consolidated and had high porosity because there was only a small amount of silica cement holding the spheres together but not filling the pore spaces. These samples continued to produce Class-2 spectra when crushed, irrespective of grain size.

[20] Crushing of the well consolidated samples had no effect on the spectra until the grains were <74  $\mu\text{m}$ , when they became optically thin, whereas the poorly consolidated samples consisted of poorly cemented silica spheres (smaller than <74  $\mu\text{m}$ ), and crushing had little effect on the bulk of the material. Conel [1969] and Salisbury and Eastes [1985] argued that attenuation of the Reststrahlen bands for fine-grained material was due to particle size and only indirectly (but critically) to porosity. The comparison of the peaks at 7.90 and 9.00  $\mu\text{m}$  in Class-1 (Figure 2c), compared to those in Class-2 show this attenuation.

## 4. Relevance for Mars Exploration

[21] The thermal emission spectrum of opal-A presented by Michalski *et al.* [2003] corresponds to the Class-1 opal-A spectrum presented herein. The Class-2 opal-A spectrum, which has been collected from natural surfaces and relates to poorly consolidated opal-A, is currently not included in the deconvolution of Martian surface spectra. Because distinguishing between the opaline phases is difficult spectrally, the addition of the Class-2 opal-A spectrum, which is distinct and unique, may assist in the identification of hydrothermal systems on the surface of Mars.

## 5. Conclusions

[22] A detailed study of the spectral properties of opal-A from the Ohaaki Pool spring system has provided the following conclusions:

[23] • “OH” exists as isolated and H-bonded  $\text{H}_2\text{O}$  molecules, and as isolated or H-bonded silanol.

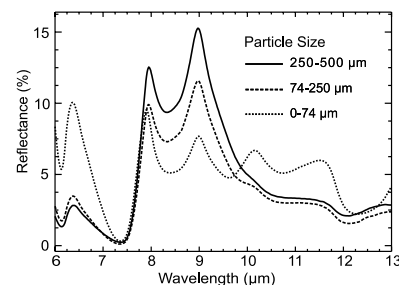


**Figure 3.** Three spectra from NZ152 between the wavelengths of 6–13  $\mu\text{m}$ , from three grain size fractions (0–74  $\mu\text{m}$ , 74–250  $\mu\text{m}$ , and 250–500  $\mu\text{m}$ ). Measurements were collected using a Nicolet Nexus 870 FT-IR Spectrometer (1.8–26  $\mu\text{m}$ ).

[24] • Two classes of opal-A spectra exist between 6–13  $\mu\text{m}$ . The Class-1 spectrum resembles the generally accepted spectrum for opal-A, which is presented by Michalski *et al.* [2003]. The Class-2 spectrum is distinct from the Class-1 spectrum and other silica polymorphs, and was collected from poorly consolidated samples.

[25] • The Class-2 opal-A spectrum should be included in the investigations of planetary surfaces, particularly those with an interest in locating siliceous hydrothermal environments.

[26] **Acknowledgment.** This research was funded by the National Science and Engineering Research Council of Canada (grant A6090 to Jones and grant 194260 to Rivard), and the Canadian Space Agency.

## References

- Adams, S. J., G. E. Hawkes, and E. H. Curzon (1991), A solid state  $^{29}\text{Si}$  nuclear magnetic resonance study of opal and other hydrous silicas, *Am. Mineral.*, *76*, 1863–1871.
- Aines, R. D., and G. R. Rossman (1984), Water in minerals? A peak in the infrared, *J. Geophys. Res.*, *89*(B6), 4059–4071.
- Chester, R., and H. Elderfield (1968), The infrared determination of opal in siliceous deep-sea sediments, *Geochim. Cosmochim. Acta*, *32*, 1128–1140.
- Conel, J. E. (1969), Infrared emissivities of silicates: Experimental results and a cloudy atmosphere model of spectral emission from condensed particulate mediums, *J. Geophys. Res.*, *74*(6), 1614–1623.
- Dijkstra, T. W., R. Duchateau, R. A. van Santen, A. Meetsma, and G. P. A. Yap (2002), Silsesquioxane models for geminal silica surface silanol sites: A spectroscopic investigation of different types of silanols, *J. Am. Chem. Soc.*, *124*, 9856–9864.
- Frondel, C. (1982), Structural hydroxyl in chalcedony (type B quartz), *Am. Mineral.*, *67*, 1248–1257.
- Gibbs, G. V. (1982), Molecules as models for bonding in silicates, *Am. Mineral.*, *67*, 421–450.
- Hunt, G. R. (1977), Spectral signatures of particulate materials in the visible and near infrared, *Geophysics*, *42*(3), 501–513.
- Hunt, G. R., and J. W. Salisbury (1970), Visible and near-infrared spectra of minerals and rocks: I. Silicate minerals, *Mod. Geol.*, *1*, 283–300.
- Hunt, G. R., J. W. Salisbury, and C. J. Lenhoff (1973), Visible and near-infrared spectra of minerals and rocks: VI. Additional silicates, *Mod. Geol.*, *4*, 85–106.
- Jones, B., and R. W. Renaut (2004), Water content of opal-A: Implications for the origin of laminae in geyserite and sinter, *J. Sediment. Res.*, *74*(1), 117–128.
- Jones, B., R. W. Renaut, and M. R. Rosen (1998), Microbial biofacies in hot-spring sinters: A model based on Ohaaki Pool, North Island, New Zealand, *J. Sediment. Res.*, *68*(3), 413–434.
- Langer, K., and O. W. Florke (1974), Near infrared absorption spectra ( $4000\text{--}9000\text{ cm}^{-1}$ ) of opals and the role of “water” in these  $\text{SiO}_2 \cdot n\text{H}_2\text{O}$  minerals, *Fortschr. Mineral.*, *52*, 17–51.
- Lyon, R. J. P. (1967), Infrared absorption spectra, in *Physical Methods in Determinative Mineralogy*, edited by J. Zussman, pp. 371–403, Academic, San Diego, Calif.
- Mahon, W. A. J., and J. B. Finlayson (1972), The chemistry of the Broadlands geothermal area, New Zealand, *Am. J. Sci.*, *272*, 48–68.
- McDonald, R. S. (1958), Surface functionality of amorphous silica by infrared spectroscopy, *J. Phys. Chem.*, *62*, 1168–1178.
- Michalski, J. R., M. D. Kraft, T. Diedrich, T. G. Sharp, and P. R. Christensen (2003), Thermal emission spectroscopy of the silica polymorphs and consideration for remote sensing of Mars, *Geophys. Res. Lett.*, *30*(19), 2008, doi:10.1029/2003GL018354.
- Milkey, R. G. (1960), Infrared spectra of some tectosilicates, *Am. Mineral.*, *45*, 990–1007.
- Moenke, H. H. W. (1974), Silica, the three dimensional silicates, borosilicates and beryllium silicates, in *The Infrared Spectra of Minerals*, edited by V. C. Farmer, pp. 365–382, Mineral. Soc., London, U. K.
- Pauling, L. (1980), The nature of the silicon-oxygen bond, *Am. Mineral.*, *65*, 321–323.
- Rodgers, K. A., et al. (2004), Silica phases in sinters and residues from geothermal fields of New Zealand, *Earth Sci. Rev.*, *66*, 1–61.
- Salisbury, J. W., and J. W. Eastes (1985), The effect of particle size and porosity on spectral contrast in the mid-infrared, *Icarus*, *64*, 586–588.
- Salisbury, J. W., and L. S. Walter (1989), Thermal infrared (2.5–13.5  $\mu\text{m}$ ) spectroscopic remote sensing of igneous rock types on particulate planetary surfaces, *J. Geophys. Res.*, *94*(B7), 9192–9202.
- Salisbury, J. W., D. M. D’Aria, and E. Jarosewich (1991a), Mid infrared (2.5–13.5  $\mu\text{m}$ ) reflectance spectra of powdered stony meteorites, *Icarus*, *92*, 280–297.
- Salisbury, J. W., L. S. Walter, N. Vergo, and D. M. D’Aria (1991b), *Infrared (2.1–25  $\mu\text{m}$ ) Spectra of Minerals*, Johns Hopkins Univ. Press, Baltimore, Md.
- Smith, J. V., and S. W. Bailey (1963), Second review of Al-O and Si-O tetrahedral distances, *Acta Crystallogr.*, *16*, 801–811.
- Sun, M. S. (1962), Tridymite (low form) in some opal of New Mexico, *Am. Mineral.*, *47*, 1453–1455.
- Takamura, T., H. Yoshida, and K. Inazuka (1964), IR characteristic bands of highly dispersed silica, *Kolloidzeitschrift*, *195*, 12–16.

B. Jones, M. C. Goryniuk, and B. A. Rivard, Department of Earth and Atmospheric Sciences, University of Alberta, 1-26 Earth Sciences Building, Edmonton, AB, Canada T6G 2E9. (benoit.rivard@ualberta.ca)